

MEASURING THE DYNAMIC SHEAR MODULUS OF POROELASTIC FOAMS IN THE AUDIBLE FREQUENCY RANGE.

G. Jansens Laboratorium voor Akoestiek en Thermische Fysica, K.U.Leuven, Belgie
L. Boeckx Laboratorium voor Akoestiek en Thermische Fysica, K.U.Leuven, Belgie
G. Vermeir Laboratorium voor Akoestiek en Thermische Fysica, K.U.Leuven, Belgie
W. Lauriks Laboratorium voor Akoestiek en Thermische Fysica, K.U.Leuven, Belgie
J. F. Allard Laboratoire d'Acoustique, Université du Maine, France

1 INTRODUCTION

The prediction of the acoustical properties of multilayered systems, including poroelastic layers using the full Biot theory¹ is limited by the absence of material data. One of the parameters that is difficult to measure is the dynamic rigidity of the porous frame. Current measurement methods^{2,3,4} are limited to the low audible frequency range (typically below 400 Hz) and require special shapes of the sample (cube, cylindrical rod or very thin samples).

Recently a new method for the measurement of the dynamic shear modulus of the frame of poroelastic foams in the medium and high audible frequency range (1 to 4 kHz) is presented⁵. This method is based on the measurement of the velocity and the damping of a Rayleigh-type surface wave on a sample of semi-infinite thickness using a laser-doppler vibrometer. The velocity of this wave is closely related to the shear velocity, which is directly linked to the shear modulus. The damping of the Rayleigh-type wave can be used to determine the imaginary part of the shear wave. The surface wave is excited through direct mechanical excitation of the frame.

At the moment a first attempt is made to measure the dynamic shear modulus on a layer of finite thickness. In this way there is no requirement whatsoever about the shape of the sample under investigation. Simulations and results of measurements are discussed.

2 RAYLEIGH WAVES ON AN ELASTIC SUBSTRATE.

At the interface between a semi-infinite elastic substrate and vacuum, a Rayleigh wave can propagate. This is a surface wave without dispersion that propagates parallel to the surface and has an amplitude that decreases exponentially with depth. The Rayleigh wave may be attenuated due to material damping in the substrate. If the vacuum is replaced with air, the surface wave can radiate energy in the upper medium, but due to the small impedance of air this effect can be neglected.

The wave number of Rayleigh waves can be expressed as a function of Poisson's ratio by the following approximate formula⁶:

$$\frac{k_R}{k_s} = \frac{0.87 + 1.12 \nu}{1 + \nu}, \quad (1)$$

with k_R and k_s the wave number of the Rayleigh wave and the shear wave respectively, and ν Poisson's ratio, which lies in the range from 0 to 0.5. For most materials, ν lies between 0.2 and 0.3. The propagation constant of the shear wave depends on the shear modulus N through:

$$k_s = \frac{\omega}{c_s} = \frac{\omega}{\sqrt{\frac{N}{\rho}}}, \quad (2)$$

with ω the angular frequency, c_s the phase velocity of the shear wave and ρ the density of the porous material.

To take into account the damping of the elastic wave, complex elastic moduli are commonly used

$$N = N_0 (1 + j\eta) \quad (3)$$

which results in a complex k_s and k_R .

From the measurement of the phase velocity of the Rayleigh wave, the real part of k_R can be obtained. The imaginary part of k_R can be estimated from the measurement of the amplitude of the surface wave at different distances from the excitation point, since the amplitude of a surface wave excited in a point decreases like $1/\sqrt{r} \exp(r \operatorname{Im}(k_R))$ with r the distance from the excitation point.

3 RAYLEIGH WAVES ON A POROUS SUBSTRATE.

Rayleigh waves on elastic substrates are commonly known and used for material research and non destructive evaluation. Surface waves on poroelastic substrates are expected to be more complex due to presence of three bulk waves (two compressional waves and a shear wave) and the interaction between fluid and solid part of the porous material. Many theoretical studies of the surface waves at fluid-filled saturated porous layer interfaces have been performed using the Biot theory. See for instance the work by Feng and Johnson⁷ and the references therein. Most of these studies were concerned with sintered glass beads and synthetic or natural sandstones saturated with liquids.

We are considering high porosity plastic sound absorbing foams in the audible frequency range with an open surface and in contact with air. For such materials, the density of the porous frame is much larger than the density of air, and in the medium- and highfrequency range the shear wave and one of the compressional waves are very similar to the shear wave and the compressional wave that propagate in an elastic solid having the same density and the same rigidity. These waves have their energy mainly in the solid part of the porous material and the fluid moves simultaneously with the solid part⁸. Dispersion and attenuation of these waves is due to a possible visco-elastic nature of the frame. The waves can easily be created by a mechanical excitation of the frame. The other compressional wave propagates mainly in the air saturating the porous medium, the frame being too heavy to move under the effect of an aerial excitation. Due to the thermal and viscous exchanges with the frame, this wave always has a dispersive nature and its phase velocity goes to a constant value at high frequencies. Surface waves at an air-air saturated porous material interface with a motionless frame have been studied previously^{9,10,11}. In the present work, the full Biot theory, taking into account the vibrations of the frame, is used to predict the phase velocity of a Rayleigh-type surface wave. The losses due to the thermal exchanges and viscous interactions between air and frame and the intrinsic damping in the porous frame are taken into account. The phase velocity and attenuation of this Rayleigh-type surface wave is used to determine the shear modulus as a function of position and direction.

For high porosity air filled porous materials the elastic constants in the Biot equations can be approximated by:

$$\begin{aligned} P &= \frac{4}{3}N + K_b + \frac{(1-h)^2}{h}K_f, \\ Q &= (1-h)K_f, \\ R &= hK_f. \end{aligned}$$

N is the shear modulus, K_b the bulk modulus of the frame, h is the porosity and K_f is the incompressibility of the air in the pores. Due to the thermal exchanges with the frame, K_f becomes frequency dependent, being equal to its isothermal value at low frequencies and to its adiabatic value at high frequencies. Several equations to account for this frequency dependence exist in literature^{8,12}. We use the formulation given by Champoux and Allard:

$$K_f = \frac{\gamma P_0}{\left\{ \gamma - (\gamma - 1) \left[1 + \frac{8\eta}{i\Lambda'^2 \operatorname{Pr} \omega \rho_0} \left(1 + i \frac{\rho_0 \omega \operatorname{Pr} \Lambda'^2}{16\eta} \right)^{1/2} \right]^{-1} \right\}},$$

with P_0 the static atmospheric pressure, γ the ratio of the specific heats, η the viscosity, Pr the Prandtl number, ρ_0 the density of air and Λ' the thermal characteristic dimension.

Due to the viscous interaction, the inertial parameters in the Biot equations also become frequency dependent. Again, several models exist to take this frequency dependence into account. We use a model due to Johnson⁸ given by:

$$\begin{aligned}\tilde{\rho}_{11} &= \rho_1 + \rho_a - i\sigma h^2 \frac{G(\omega)}{\omega}, \\ \tilde{\rho}_{12} &= -\rho_a + i\sigma h^2 \frac{G(\omega)}{\omega}, \\ \tilde{\rho}_{22} &= h\rho_0 + \rho_a - i\sigma h^2 \frac{G(\omega)}{\omega},\end{aligned}$$

where:

$$\begin{aligned}\rho_a &= h\rho_0(\alpha_\infty - 1), \\ G(\omega) &= \left(1 + \frac{4i\alpha_\infty^2 \eta \rho_0 \omega}{\sigma^2 \Lambda^2 h^2}\right)^{1/2}.\end{aligned}$$

α_∞ is the tortuosity, σ the flow resistivity and Λ the viscous characteristic dimension. The wave numbers of the two compressional waves and the shear wave are given by:

$$\begin{aligned}k_1^2 &= \frac{\omega^2}{2(PR - Q^2)}(P\tilde{\rho}_{22} + R\tilde{\rho}_{11} - 2Q\tilde{\rho}_{12} + \sqrt{D}), \\ k_2^2 &= \frac{\omega^2}{2(PR - Q^2)}(P\tilde{\rho}_{22} + R\tilde{\rho}_{11} - 2Q\tilde{\rho}_{12} - \sqrt{D}), \\ k_3^2 &= \frac{\omega^2}{N} \left(\frac{\tilde{\rho}_{11}\tilde{\rho}_{22} - \tilde{\rho}_{12}^2}{\tilde{\rho}_{22}} \right) \\ D &= (P\tilde{\rho}_{22} + R\tilde{\rho}_{11} - 2Q\tilde{\rho}_{12})^2 - 4(PR - Q^2)(\tilde{\rho}_{11}\tilde{\rho}_{22} - \tilde{\rho}_{12}^2).\end{aligned}$$

Each wave type has an amplitude in the solid and the fluid part of the porous material. The ratios of the amplitudes of the displacements of each wave in air and frame are given by:

$$\begin{aligned}\mu_i &= \frac{Pk_i^2 - \omega^2 \tilde{\rho}_{11}}{\omega^2 \tilde{\rho}_{12} - Qk_i^2}, \quad i = 1, 2, \\ \mu_3 &= -\frac{\tilde{\rho}_{12}}{\tilde{\rho}_{22}}.\end{aligned}$$

We used a sound absorbing material called "Fireflex", manufactured by RECTICEL, Wetteren, Belgium. The parameters of this material have been measured independently^{13,14,15,16} and are given in Table 1.

Tortuosity α_∞	Flow resistivity σ Ns/m ⁴	Porosity h	Viscous dimension Λ μm	Thermal dimension Λ μm	density ρ_1 kg/m ³	Shear modulus N N/m ²	Poisson Ratio ν
1.4	50000	0.98	50	150	25	(0.75+i0.15)10 ⁹	0.3

Table 1. Parameters of the material used in the simulations and the measurements.

When we calculate the wavenumbers, for instance at a frequency of 2 kHz, and compare them with the wavenumbers of a hypothetical solid elastic material with the same density and elastic constants as the porous material, the results are as given in Table 2.

	elastic porous material	equivalent elastic solid material
k_1 (air-borne compressional)	$70.0 - i 36.1 \text{ m}^{-1}$	-
k_2 (frame-borne compressional)	$118.9 - i 24.1 \text{ m}^{-1}$	$120.9 - i 12 \text{ m}^{-1}$
k_3 (shear)	$230.6 - i 24.0 \text{ m}^{-1}$	$226 - i 22.4 \text{ m}^{-1}$

Table 2. wavenumbers at 2kHz for the three waves in the porous material and the two waves in an elastic solid material.

The real part of the wavenumbers is very close to each other. The imaginary parts of the wavenumbers of the porous material are larger. This is mainly due to the interaction with the fluid in the porous material. This means that for practical purposes, for determining the shear modulus from the phase velocity of the Rayleigh wave, the more simple equations from paragraph 2 can be used instead of the full poroelastic model.

Surface waves are associated with poles of the reflection coefficient (a 'reflected' wave can exist without 'incident' wave). The reflection coefficient is given by:

$$R(\sin \theta) = \frac{Z_s(\sin \theta) - \rho_0 c_0 / \cos \theta}{Z_s(\sin \theta) + \rho_0 c_0 / \cos \theta}.$$

c_0 being the phase velocity in free air and Z_s the surface impedance of a semi-infinite layer. It is convenient to plot the reflection coefficient in the complex $\sin \theta$ plane. The real axis corresponds to the reflection coefficient at different angles of incidence as measured with different methods. The interval $0 \leq \sin \theta \leq 1$ corresponds with plane incident waves at real angles of incidence. Consequently, due to considerations of conservation of energy, the reflection coefficient should be smaller than 1 on this interval. The interval $1 \leq \sin \theta \leq \infty$ corresponds to inhomogeneous incident waves where planes of constant phase and planes of constant amplitude do not coincide. As a consequence, the reflection coefficient can be larger than 1 in this interval.

When a pole is present at $\sin \theta_p$ in the area $1 \leq \text{Re}(\sin \theta) \leq \infty$, $0 \leq \text{Im}(\sin \theta)$, it can cause a sharp maximum of the reflection coefficient on the real $\sin \theta$ axis at a location close to $\text{Re}(\sin \theta_p)$. The closer this pole is located to the real $\sin \theta$ axis, the larger the peak in the reflection coefficient will be. Using the stress-strain relations for a poroelastic material and the continuity of stress and displacements at the interface of a semi-infinite layer, the surface impedance Z_s can be evaluated numerically. Calculations show only one pole close to the real $\sin \theta$ axis associated with a proper surface mode, the other poles being too far from the real $\sin \theta$ axis to result in observable surface modes. Table 3 shows the horizontal component of the wavenumber of the surface wave at 2 kHz together with the result obtained from equation 1.

k_R from position of pole of $R(\sin \theta)$	k_R from equation 1
$247.7 - i 25.7 \text{ m}^{-1}$	$243.7 - i 24.1 \text{ m}^{-1}$

Table 3. Wavenumber of the Rayleigh wave.

4 EXPERIMENTAL PROCEDURE

Observation of a surface wave related to the air-borne wave above a thin layer of rigid porous material have been done in the past using a point source above the layer^{10,11}. Calculations show that the energy of the point source seldom couples to the frame-borne wave and the shear wave in the porous material and in most cases only the air-borne wave is excited noticeably. However, The frame borne wave is excited easily using direct mechanical excitation of the frame using for instance a shaker.

Similar to a point source in air, a vertical periodic point force acting on the frame can be written as the sum of axisymmetric components:

$$F \delta(r) = \frac{Fk^2}{2\pi} \int_0^\infty J_0(k\xi r) \xi d\xi.$$

The velocity of the frame at a point located at a distance r from the source is given by:

$$v_z^s(r) = \frac{Fk^2}{2\pi} \int_0^\infty J_0(k\xi r) V_z^s(\xi) \xi d\xi.$$

The transfer function V_z^s can be calculated⁵ in a similar way as the reflection coefficient of the layer. Similar equations for the vertical velocity component of the air above the surface and for the pressure in the air in a point near the surface can be obtained. It can be shown that the poles of the transfer function V_z^s are the same as the poles of the reflection coefficient⁵.

Figure 1 shows schematically the experimental setup. A thick (20 cm) block of foam is placed on a rigid surface. At frequencies of 2 kHz and higher, the wavelength of the surface wave is 2.5 cm or smaller and the block can be considered as semi-infinite. A LDS shaker is attached to the foam with a small piece of double-sided tape. The displacement is measured with small KNOWLES accelerometers attached to the foam or with a Polytec vibrometer, where the laser beam is directed towards the foam surface with a small mirror. A small (a few square millimeter) patch of retroreflecting tape is attached to the foam to get a good signal to noise ratio of the vibrometer.

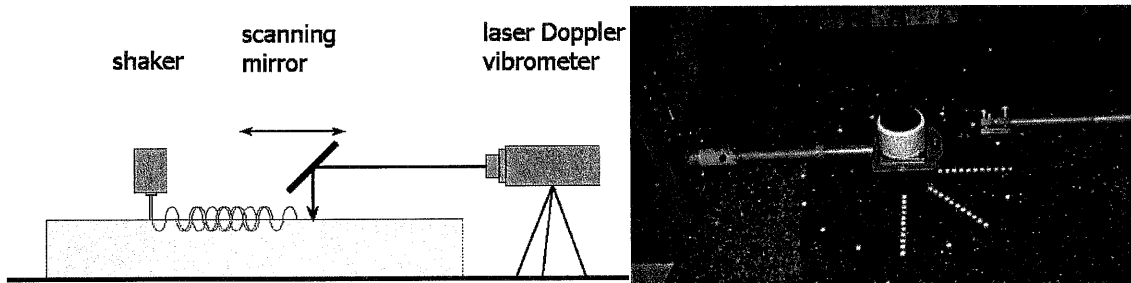


Figure 1. Experimental setup with the shaker, scanning mirror and vibrometer (not shown in the photo).

The shaker generates a sine burst with a few cycles centered on a frequency. Figure 2 shows two different recorded signals at two different distances from the source together with the crosscorrelation function used to measure the travel time. From the travel time, the phase velocity of the surface wave can be calculated and from the amplitude of the recorded signal, the imaginary part of the propagation constant can be calculated.

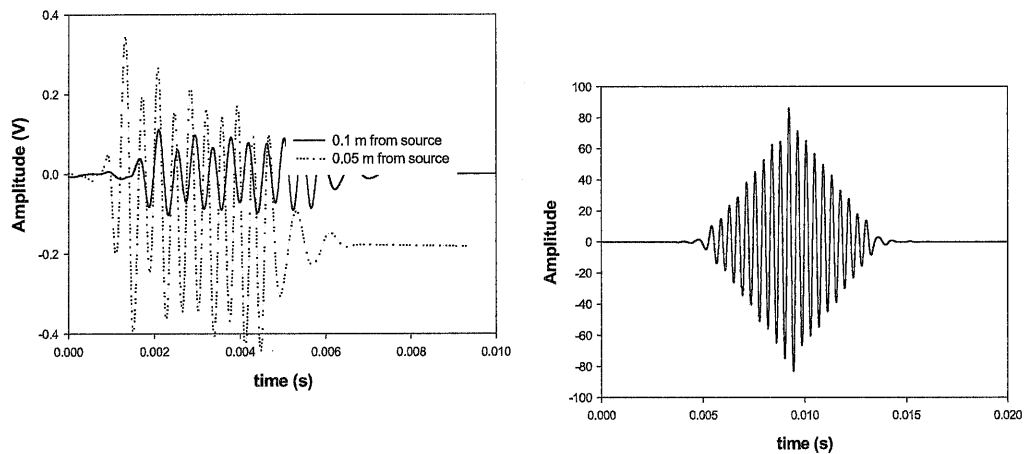


Figure 2. Recorded waveforms at two different locations and the crosscorrelation function.

Plotting the arrival time and the amplitude of the burst as a function of distance to the source results in a precise estimate of the phase velocity and attenuation of the Rayleigh wave at the center frequency of the burst signal. Figure 3 shows the regression curves for a frequency of 2.4 kHz.

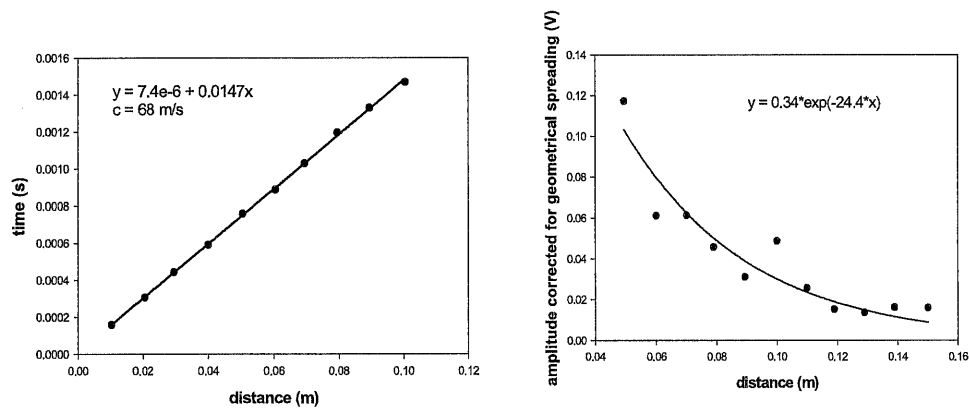


Figure 3. Experimental results at 2.4 kHz. Left: time of flight, right: attenuation.

The Table 2 gives the results for two different frequencies. The shear modulus has been extracted from the results using equation 1.

frequency (kHz)	phase velocity (m/s)	$\text{Re}(k_{\text{Rayleigh}})$ m^{-1}	$\text{Im}(k_{\text{Rayleigh}})$ m^{-1}	Shear modulus (N/m^2)
2.4	68.0 ± 0.5	222 ± 2	-24 ± 3	$(1.55 + i0.34)10^5$
3.0	68.0 ± 0.5	277 ± 2	-33 ± 3	$(1.56 + i0.38)10^5$

Table 2. Experimental results.

The shear modulus in Table 2 has been obtained assuming a typical Poisson ratio of 0.3, but in any case the result of equation 1 is rather insensitive to the value of the Poisson ratio.

One advantage of the present method over the traditional methods for determining the elastic coefficients of plastic foams is that the sample does not need to be manipulated and cut into specific shapes. Indeed, the latter may very well damage the cell structure of the foam, resulting in biased data. Plastic foams used for sound absorption are often viscoelastic. As a result, their elastic moduli increase with frequency (these materials can be 'soft' at low frequency and more rigid at higher frequency). Traditional methods are based on the measurement of a resonance in a beam or

a bar and can only give good results at low (typically < 100 Hz) frequencies. With the present method, it is easy to obtain the elastic coefficient in the audible frequency range. Moreover, information on the frequency dependence of the shear modulus can be obtained.

Due to the fabrication process¹⁶ (a liquid melt starts foaming and rises in the vertical direction), the foams elastic properties are orthotropic: the elastic coefficients in the vertical direction being different from those in a horizontal plane. The present method was used to measure the shear modulus as a function of the direction along the surface for two different blocks: one cut in the vertical direction and another cut in the horizontal direction. Since the measurements are performed along the main axes of the anisotropic material, pure modes will still exist in each direction. The results are given in Figure 4 and clearly show the anisotropic nature of the foam.

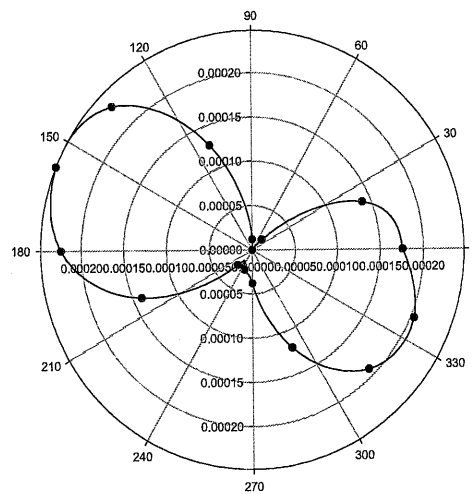


Figure 4: Variation of arrival time of the burst as a function of direction in the surface of the foam. Block cut in a the vertical direction, parallel to the direction in which the foam rises during production.

5 CONCLUSIONS

A Rayleigh-like surface wave can be observed at an air- air saturated porous layer interface. This Rayleigh wave has been modeled using the full Biot model for poroelastic media, but a simpler model based on an elastic solid with the same density and elastic coefficients as the foam nearly gives the almost same results. The dynamic shear modulus can be determined from the phase velocity of this surface wave at higher frequencies, which are relevant for different applications modeling sound absorbing materials. There are no requirements for the shape of the sample; only a sufficient thick slab is needed. Damping can be estimated from the exponential decay of this surface wave. Possible anisotropy can easily be observed. The method can be extended to the low frequency region, where the block can no longer be considered as a semi-infinite medium, by taking the reflection from the bottom into account.

6 REFERENCES

- 1) M.A. Biot, "Theory of propagation of elastic waves in a fluid-saturated porous solid", *Journal of the Acoustical Society of America*. **28**, 1956, 168-191.
- 2) L. Kelders et al., "Experimental study of the dynamic elastic moduli of porous materials", *Proceedings of the 11th FASE symposium*, 1994, 19-22.
- 3) E. Mariez et al., "Elastic constants of polyurethane foam's skeleton for Biot model", *Proceedings InterNoise*, 1996, 951-954.
- 4) M.Melon, E.Mariez, C.Ayrault, S.Sahraoui "Acoustical characterization of open-cell foams" *Journal of the Acoustical Society of America* **104** , 2622-2627 (1998)
- 5) J.F. Allard, G. Jansens, G. Vermeir, and W. Lauriks, "Frame-borne surface waves in air saturated porous media", *Journal of the Acoustical Society of America* **111**, 2002, 690-696
- 6) I.A.Victorov, Rayleigh and Lamb waves (Plenum, New York, 1967)
- 7) S.Feng and D.L.Johnson "High-frequency acoustic properties of a fluid/porous solid interface. I New Surface mode. *Journal of the Acoustical Society of America* **74**, 906-924 (1983)
- 8) J.F.Allard, *Propagation of Sound in Porous Media - Modeling Sound Absorbing Materials* (Chapman&Hall, London, 1993)
- 9) Tizianel, J., Allard, J. F., Lauriks, W., and Kelders, L., "Experimental localization of a pole of the reflection coefficient of a porous layer" *Journal of Sound and Vibration* **202** (1997) p.600-604.
- 10) Kelders, L., Lauriks, W., and Allard, J. F., "Surface waves above thin porous layers at ultrasonic frequencies" *Journal of the Acoustical Society of America* **104** (1998) p.882-889.
- 11) W.Lauriks, L.Kelders, J.F.Allard "Surface waves and Leaky waves above a porous layer" *Wave Motion* **28**, 59-67 (1998)
- 12) K.Attenborough, "Acoustical characteristics of porous materials" *Physics Reports-Review Section of Physics Letters* **82** (1982) p.179-227.
- 13) Leclaire, Ph., Kelders, L., Lauriks, W., Melon, M., Brown, N., and Castagnede, B., "Determination of the viscous and thermal characteristic lengths of plastic foams by ultrasonic measurements in helium and air" *Journal of Applied Physics* **80** (1996) p.2009-2012.
- 14) Leclaire, Ph., Kelders, L., Lauriks, W., Allard, J. F., and Glorieux, C., "Ultrasonic wave propagation in reticulated foams saturated by different gases - high frequency limit of the classical models" *Applied Physics Letters* **69** (1996) p.2641-2643.
- 15) Leclaire, Ph., Kelders, L., Lauriks, W., Glorieux, C., and Thoen, J., "Determination of the viscous characteristic length in air filled porous materials by ultrasonic attenuation measurements" *Journal of the Acoustical Society of America* **99** (1996) p.1944-1948.
- 16) Allard, J. F., Castagnede, B., Henry, H., and Lauriks, W., "Evaluation of tortuosity in acoustic porous materials saturated by air" *Review of Scientific Instruments* **65** (1994) p.754-755.
- 17) L.J.Gibson, F.M.Ashby *Cellular Solids, Structure and Properties* (Pergamon, Oxford, 1988)